Surface Plasmon–Coupled Emission: What Can Directional Fluorescence Bring to the Analytical Sciences?

Shuo-Hui Cao, Wei-Peng Cai, Qian Liu, and Yao-Qun Li

Department of Chemistry and Key Laboratory of Analytical Sciences, College of Chemistry and Chemical Engineering, Xiamen University, Xiamen 361005, China; email: yqlig@xmu.edu.cn

Annu. Rev. Anal. Chem. 2012. 5:317–36

First published online as a Review in Advance on April 9, 2012

The *Annual Review of Analytical Chemistry* is online at anchem.annualreviews.org

This article's doi: 10.1146/annurev-anchem-062011-143208

1936-1327/12/0719-0317$20.00

Keywords

optics, plasmonics, luminescence, DNA, immunoassay, sensing

Abstract

Surface plasmon–coupled emission (SPCE) arose from the integration of fluorescence and plasmonics, two rapidly expanding research fields. SPCE is revealing novel phenomena and has potential applications in bioanalysis, medical diagnostics, drug discovery, and genomics. In SPCE, excited fluorophores couple with surface plasmons on a continuous thin metal film; plasmophores radiate into a higher–refractive index medium with a narrow angular distribution. Because of the directional emission, the sensitivity of this technique can be greatly improved with high collection efficiency. This review describes the unique features of SPCE. In particular, we focus on recent advances in SPCE-based analytical platforms and their applications in DNA sensing and the detection of other biomolecules and chemicals.

1. INTRODUCTION

Surface plasmon: collective and periodic free-electron oscillation at the surface of a conductor

SPR: surface plasmon resonance

SPCE: surface plasmon–coupled emission

***p* polarization:** linear polarization; the magnetic vector is perpendicular to the plane of incidence and the electric vector affects the sample surface

Fluorescence detection has been widely used in numerous biochemical assays, and its high sensitivity has made such detection successful even at the single-molecule level (1). However, challenges remain regarding demands from the fields of bioanalysis, genetic engineering, clinical diagnosis, and drug screening for techniques that can achieve high sensitivity and selectivity. Metallic materials, including particles and films at the nanometer level, reveal special optical phenomena when plasmons interact with molecules in the near field; techniques to reveal these phenomena include surface plasmon resonance (SPR), localized surface plasmon resonance (LSPR), and surface-enhanced Raman scattering (SERS), which have been extensively investigated and play important roles in sensing applications (2–3). Researchers have been studying the interactions between fluorophores and plasmons, which have recently begun to attract more attention (4–5). These attempts to integrate fluorescence and plasmonics are ushering in a revolution in the analytical sciences. Herein, we introduce a novel fluorescence-engineering technology known as surface plasmon–coupled emission (SPCE) or surface plasmon–coupled directional emission. This technique, first described by Lakowicz et al. (6–8), successfully combines fluorescence and SPR. The sensitivity can be greatly increased, and the unique properties of this approach are useful for the development of novel analytical methods (9).

First, we describe the mechanism of SPCE, summarize its special optical characteristics, and discuss the features that are important for analytical chemistry. Second, we describe present efforts to improve SPCE as a useful analytical tool. We discuss progress in analytical strategies and optical imaging techniques based on SPCE. Third, we provide examples of the analytical applications that demonstrate the significant success of SPCE. Finally, we discuss the outlook and prospective trends of this technique.

2. THE FUNDAMENTALS OF SURFACE PLASMON–COUPLED EMISSION

SPCE occurs when excited fluorophores are positioned up to 200 nm above a continuous thin metallic film approximately 20 to 50 nm thick. To satisfy wave-vector matching, the fluorophores can couple with the metal surface to cause the oscillation of surface plasmons, and the energy can then be released as radiation (10). Remarkably, the emission can be observed from the film through a prism attached to its back, but only at a unique angle measured from the normal to the interface. Because the fluorophores are symmetrically distributed around the normal, the emission is observed as a cone around it (**Figure 1*a***). This phenomenon differs from traditional fluorescence, wherein the spatial distribution is isotropic. This emission has the same spectrum as that from fluorophores, so it can be considered as originating from the fluorophores. However, the emission is highly *p* polarized no matter what the polarization of the excitation light is, which indicates that the emission should reflect properties of the surface plasmons. Both fluorophores and surface plasmons contribute to such complex emission, so more information can be obtained. The emitting species are termed plasmophores.

The fundamentals of SPCE are related to those of SPR (10). **Figure 1*a*** illustrates the process of light incidence and reflection in SPR. The light impinges on the gold film through a prism, and the reflected light can be monitored. In SPR, only *p*-polarized light with a perpendicular electric field can excite surface plasmons, which are bound in the perpendicular direction. At the same time, the specific condition that the elements of wave vectors propagating along the interface between metal and another medium be equal should be satisfied. However, the wave vector of light in free space (k_0) is usually smaller than the wave vector of surface plasmons propagating along

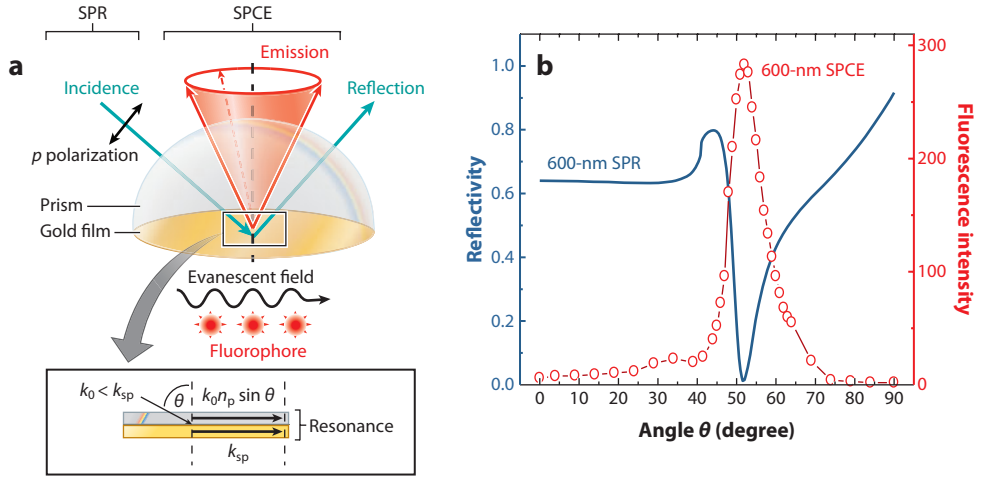

Figure 1

(*a*) Surface plasmon resonance (SPR) and surface plasmon–coupled emission (SPCE) on a prism configuration. (*Inset*) The resonance of surface plasmons arising from the matching of wave vectors on the interface. (*b*) Calculated SPR reflectivity (*blue line*) and SPCE fluorescence (*red line*) angular distributions of a sulforhodamine 101–doped poly(vinyl alcohol) film spin-cast to a gold film–coated substrate attached to a prism. The calculated simulation can be achieved by resolving the multilayer Fresnel equation.

the interface (k_{sp}), so a higher–refractive index material, typically a glass prism, is used to amplify k_0 (11). If the refractive index of a prism is n_p, and light is input at an angle of θ relative to the normal of the surface, the x-axis component of the light wave vector in the prism (k_x), which lies along the metal surface, is $k_0 n_p \sin\theta$. Resonance occurs when k_x is equal to k_{sp} along the interface (**Figure 1**) (12). Therefore, a defined angle of θ can be observed for one wavelength of light in a defined system in which the parameters of k_0, n_p, and k_{sp} are exclusive. Upon resonance, the energy of the incident light is adsorbed by the excited surface plasmons, which causes a dramatic decrease in reflection. As a result, a minimum can be observed in the reflectivity curve monitored with θ, where the angle is known as the SPR angle. At other angles, the reflectivity is high for a metal surface.

SPCE can be understood by reference to the related process of SPR. The excited surface plasmons oscillate normal to the surface with the resonance of incident light, and they propagate along the surface as a wave. The intensity decreases exponentially both perpendicular and parallel to the surface due to the damped oscillation. The plasmon wave can be observed as an evanescent field distributed around ~200 nm beyond the surface (13). Within the near-field distance, the fluorophores can experience the energy field, and the excited dipoles couple strongly with the surface plasmons, thereby inducing the release of energy as radiation from the prism. This phenomenon should occur through wave-vector matching. Therefore, the radiation with *p* polarization can be released only in a direction where the prism and surface wave vectors match well (9, 14–15). If one focuses on the fluorescence intensity as it changes with the observed angle (defined as the angle relative to normal of the surface) from the prism side, one observes an obvious peak at a sharp angle, which is perfectly consistent with the SPR angle in the wavelength of emission (**Figure 1*b***). Thus, the directional emission is the result of interactions between surface plasmons and fluorophores.

On the basis of prism coupling measurements, two modes of SPCE can be used (9); the fluorophores can be excited with light incident from either the prism side or the sample side. In the first mode (through the prism), the incident light at the SPR angle can induce the oscillation of

Evanescent field: an electromagnetic field whose intensity decays exponentially with distance within hundreds of nanometers from the boundary

surface plasmons to excite the nearby fluorophores. In this mode, the device operates similarly to SPR and is known as the Kretschmann (KR) configuration. In the second mode (through the sample), the incident light can directly excite the fluorophores so that the dipoles in the near field couple to surface plasmons, thereby inducing directional emission through the prism. This mode is known as the reverse Kretschmann (RK) configuration. In the KR configuration, the excited field is greatly enhanced in a resonance with an evanescent field (5), so the SPCE intensity is much higher than in the RK configuration (16). However, the direct incidence in RK configurations means that these devices are easier to create (9). For example, a light-emitting diode (LED) has been used in low-cost designs (17), and the use of xenon light allows experimenters to choose the wavelength (18). Investigators can further enhance this technique's collection efficiency by setting up a conical mirror around the prism, which collects all of the signals of the SPCE ring by reflecting them into a point (19). A miniaturized device can be created through modification of the design of a spectrofluorometer (20). In addition to the prism coupling, the grating can also induce directional emission (21). Note that optical excitation is not essential for directional emission. SPCE can also be applied to chemiluminescent and electrochemiluminescent species (22–23). Finally, directional emission has also been observed as forms of phosphorescence and two-photon excited fluorescence (24–25).

3. THE IMPORTANT PROPERTIES OF SURFACE PLASMON–COUPLED EMISSION

Due to its unique properties, SPCE has attracted a great deal of interest in recent years (26). Here, we briefly summarize and analyze the main properties of SPCE. We focus on those properties that are potentially important for the development of novel analytical methods.

3.1. Directional Emission

An important characteristic of SPCE is directional emission, which means that nearly all of the signal is concentrated into a single direction. Thus, one can achieve a high rate of collection simply by pointing a detector in the defined direction. Directional emission is important in increasing sensitivity; a 50-fold increase is expected with high collection efficiency, compared with isotropic spontaneous fluorescence. In the KR configuration, a 10- to 40-fold-enhanced excitation field should also be considered, which would lead to an overall increase in sensitivity of up to 1,000-fold (9). This significant sensitivity enhancement has allowed investigators to develop ultrasensitive fluorescence assays to monitor extremely low concentrations of analytes; such applications are often required in biochemical and biomedical research.

The angle at which the emission radiates directionally is relevant to many optical factors, including the dielectric properties of the metal, the wavelengths of fluorophores, and the refractive index of the environment (27). Therefore, the directional angle displays different cases and contains important analytical information, which can help characterize the state of the system and the process of reaction. It also provides the opportunity to design new instrumentation. In the case of gold film, fluorophores with different emission maxima display SPCE at different angles because of the diversity of wave vectors for various wavelengths. As a result, the spectra of a mixture of fluorophores are distinct; each reflects only one fluorophore at the defined angle (10, 18). The fluorophores can be observed as a function of wavelength resolution. The wavelengths are distinguished directly through angular separation without filters, which may hold potential for miniaturized instrumentation by eliminating many optical components.

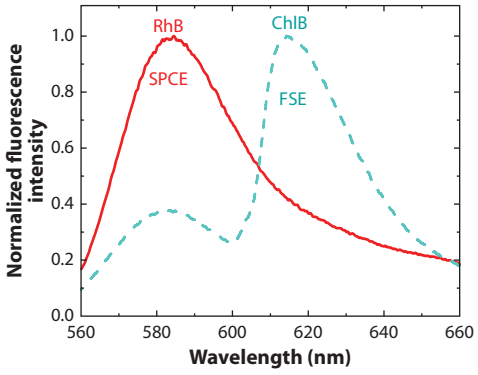

Figure 2

Normalized surface plasmon–coupled emission (SPCE) and free-space emission (FSE) spectra of 1 mM of Rhodamine B (RhB) in a 30-nm poly(vinyl alcohol) film spin-cast to a gold film, with 1 mM of Chlorophyll B (ChlB) in ethanol as a background. The reverse Kretschmann configuration was used (S.H. Cao, T.T. Xie & Y.Q. Li, unpublished data).

3.2. Background Suppression

SPCE is generated by the interaction between fluorophores and a nearby metal film. Therefore, the signal comes from the substance near the interface, whereas no signal is produced further from the surface. SPCE offers the ability to use spatial resolution to selectively detect analytes located in the near field; interference from the bulk solution is eliminated. In one experiment (**Figure 2**), Rhodamine B (RhB) was located in the near field of a gold film through spin-casting. Chlorophyll B (ChlB) was added to the bulk solution as the background. In the RK configuration, the incident light excited both RhB and ChlB directly, so both signals were observed through the detection of free-space emission (FSE) from the sample side. However, only the RhB signal was observed in the detection of SPCE, even with the high background—the signal for ChlB in the chosen concentrations was dominant in the FSE detection. More effective background suppression can be expected in the KR configuration, even with high concentration interference, because the fluorophores are selectively excited near the surface through an evanescent field (10). The practical significance of this finding is evident in analytical experiments to eliminate interference. Such advantages are attractive for clinical assays (28).

3.3. *p*-Polarized Emission

The polarization of SPCE is the most convincing evidence of coupling with surface plasmons. In a ~100-nm-thick isotropically oriented fluorophore layer, the emission is almost purely *p* polarized regardless of the polarization of the incident excitation, whereas FSE displays similar intensities for both *p* and *s* polarization (6, 10). The characteristics of *p*-polarized emission allow one to identify the coupling of surface plasmons and exclude background scattering with a polarizer. Anisotropy emission has been proven, both theoretically and experimentally, to depend on the orientation of dipoles, which are excited fluorophores that can be regarded as points (14, 29). The radiation of the vertical dipoles on the surface is purely *p* polarized, which can contribute to the coupling of surface plasmons. For horizontal dipoles along the surface, the radiation contains the components of both *s*-polarized and *p*-polarized emission (30), but only the *p*-polarized part represents the signal of SPCE. As a result, an asymmetry in the SPCE cone is observed when the dipoles are oriented horizontally; the signal is stronger in the direction parallel to the dipoles and weaker in

FSE: free-space emission

the direction perpendicular to the dipoles (29). In most cases, the orientation of the dipoles is isotropic, and the SPCE cone appears symmetrical.

Coupling efficiency: the ability of the excited fluorophores' energy to be transferred to surface plasmons, which causes directional radiation

When the fluorophore layer is thicker than 100 nm, the phenomena seem to be more complex. More than one emission ring can be observed at one wavelength in SPCE, which means that the emission no longer occurs in only one direction. The polarization and the intensity show subverted properties: A strong directional signal with *s*-polarized radiation can be observed, and the polarization alternates for rings with different dielectric thickness (31). These effects can be explained by the additional plasmon modes that exist on the metal surface (32). Considering that the thickness of the dielectric film is comparable to the wavelength, it is possible to have the admittance reverse the phase shift of *s*-polarized radiation to fit the mode of the waveguide (33–34), or the waveguide can be coupled to the plasmon resonance (35). Such multipolarization is valuable as an analytical parameter of dielectric film thickness, which usually undergoes significant changes in the course of biomolecular binding.

3.4. Distance-Determined Coupling

The coupling of SPCE is closely related to the distance between the fluorophore and the metal surface. When the fluorophore is very close to the surface, especially within 10 nm, its energy is transferred to the surface in a radiation-less form, so the quenching effect is dominant. At a distance longer than 500 nm, however, the interference between the far-field radiation and its reflection dominates (36–38). Therefore, the appropriate distance for SPCE is beyond the range of quenching but close enough (usually 20 nm to 200 nm) to the surface for the excited dipoles to couple to the surface plasmons radiating into the prism (9).

Note that the coupling efficiency of fluorophores distributed at the effective coupling distance varies, displaying an increase within 50 nm and undergoing a dramatic decrease at more than 200 nm (39–40). The position of the fluorophores plays an important role in determining the intensity of the directional radiation. The maximum of the coupling efficiency can be expected to occur at the optimized position. These properties both offer great opportunities and pose a challenge for practical (especially quantitative) analysis because it is difficult to affirm the position of fluorophores near the surface. However, once the process is completed, one can expect accurate spatial resolution, which we discuss further below.

The emission dynamics is also related to the distance. At a short distance of approximately 10 nm, SPCE decays faster than FSE, whereas at a distance greater than 20 nm, the lifetimes of both SPCE and FSE are nearly the same. This finding may be attributed to the coupling's sensitivity to the orientation of the dipole within a few nanometers, given the different components of the dipoles orienting between SPCE and FSE (41).

4. PROGRESS IN IMPROVING SURFACE PLASMON–COUPLED EMISSION

The unique properties of SPCE are applicable to the fields of analytical chemistry and biochemistry. Investigators have devoted increasing effort to enhancing this technique's capabilities. In this section, we discuss strategies for improving SPCE.

4.1. Widening the Optical Window

The general applicability of SPCE to different types of fluorophores with various excitation and emission wavelengths is significant for the development of technique platforms. Gold and silver are usually used as the films in SPR and SPCE because their free electrons can form a coherent

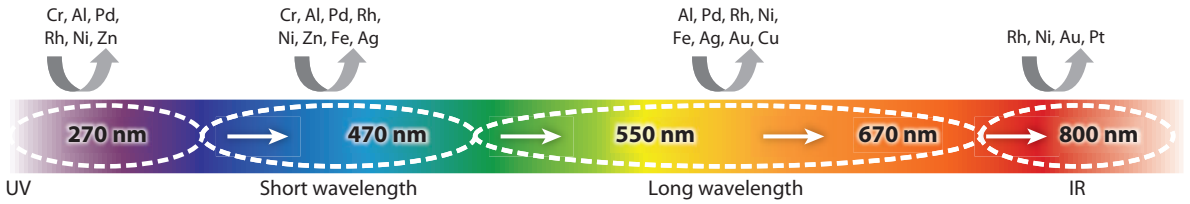

Figure 3

Metals that can be used as optical surfaces for surface plasmon–coupled emission in the UV-to-IR range.

oscillation at the electromagnetic radiation; the resonance of other metals with a large imaginary part of dielectric constants would be depressed (3). The appropriate spectral range to which gold and silver can be applied is concentrated in the red spectral region and the visible spectral region, respectively (27, 42); these ranges limit the generality of the technique in some assays, such as proteins with fluorescence in the UV range. However, some metals, including transition metals, also exhibit surface enhancement in other ranges of the spectrum. Although not very strong (43–44), this phenomenon offers promising alternatives for SPCE.

The use of various metals has been investigated in attempts to widen the optical window in which SPCE can be applied. Researchers have recently established a general procedure for the selection of a thin metal film for use in SPCE (45). Reflectivity curves, calculated by performing Fresnel equations, are useful in indicating the potential surface plasmon resonance. First, one should compare metal films of various thicknesses to determine the optimum thickness. For metals with a large imaginary part of their dielectric function, the optimum thickness is approximately 20 nm, which is less than the usual thickness of approximately 50 nm for gold and silver films. Second, one should evaluate the wavelength range matching the chosen metal through the minimum reflectivity of *p*-polarized light at the SPR angle; the value should be smaller than 0.2. Following the simulation, one can validate the possibility of using the chosen metal. Metals that can be used in SPCE include copper (46), aluminum (47), zinc (48–49), iron (18, 50–51), nickel (52), platinum (53), palladium (54), chromium (45), and rhodium (45). Note that the whole spectral region from UV to IR can now be accessed by making the appropriate selection of metal film (**Figure 3**) (45). The widened optical window makes approaches using optional fluorophores viable, so the use of alternative metals can be expected.

An advantage arising from the use of iron and palladium is fixed-angle observation, which is convenient for the combination of spectroscopic measurements (45, 54). This advantage allows one to observe the directional signal of multifluorophores with one spectral scan, which is particularly attractive in labeled systems in biological applications (18). Moreover, the penetration depth, namely the distance to which the evanescent wave reaches into the dielectric, can be manipulated through the use of different metal films (55), so the penetration depth becomes more flexible in assays. If the analytes are close to the surface and the background is strong, a metal with a short penetration depth should be used to selectively detect the analytes. When detecting large-sized analytes, especially in bioassays, a metal film with a long penetration depth should be chosen.

4.2. Enhancing the Capability of Surface Plasmon–Coupled Emission for Rapid and Sensitive Detection

Technical innovations have been implemented to improve the applicability and sensitivity of SPCE. One such technique, proposed by Geddes and coworkers (56), is known as microwave-accelerated surface plasmon–coupled emission (MA-SPCE). Both speed and sensitivity are

MEF: metal-enhanced fluorescence

paramount in clinical assays, but the molecular reactions in bioassays usually take a long time, from a few minutes to hours, which poses a problem for fast detection. Microwaves can be employed to accelerate the kinetics of molecular reactions in bioassays (57), offering the opportunity to develop fast and sensitive assays that combine elements of both microwaves and SPCE. Examples of this combination's applications to DNA hybridization and protein immunology are described in Section 5 (56, 58). Also, certain special geometrical structures with tips can be used to further enhance the microwave effect due to the intense field distributions near the tips (59).

Owing to the LSPR effect of metal nanoparticles, enhanced fluorescence from nearby fluorophores can be observed. This phenomenon is known as metal-enhanced fluorescence (MEF) (60); it can significantly affect SPCE (61). In one experiment, silver colloids with different radiuses were placed on substrates that either were or were not coated with gold films; the fluorophores were then immobilized to cover the substrates. Emissions from the prism side and the sample side were collected. The presence of silver colloids not only enhanced the FSE but also increased the intensity of SPCE. The intensity was much higher in the case of the 80-nm colloids from the back of the gold substrate, compared with the 20-nm colloids, whose radius was within the quenching limit, and the control sample without colloids. Further studies used colloidal nanoparticles to enhance the coupling efficiency of excited fluorophores to surface plasmons on smooth metal films. For a silver colloid–silver film system, the optimal colloid size was 40 nm (62). Also, silver islands deposited onto copper films caused an enhancement in SPCE (63), so it may be possible to enhance the SPCE signal from various metal films by incorporating the effect of MEF. Therefore, MEF-SPCE systems provide dramatic signal enhancement and improved photostability for both FSE and plasmon-coupled emission; these improvements could be employed to increase the sensitivity of SPCE-based assays.

4.3. Obtaining Controllable Coupling with Spatial Resolution in Surface Plasmon–Coupled Emission

As mentioned above, the coupling effect that occurs close to the metal surface is dramatically sensitive to the spatial position along the normal to the metal surface; it is the traditional fluorescence technique, which demands homogeneous distribution throughout the entire space. We must confront this challenge by finding approaches to ensure that the fluorophores under study can be uniformly distributed at the expected spatial position. Otherwise, the efficiency with which fluorophores couple to plasmons would be unpredictable and not uniform and therefore would result in false responses in assays. However, the distinct distance-dependent feature offers the possibility of monitoring the molecules around the surface with high spatial resolution through evaluation of the coupling effect.

Langmuir-Blodgett (LB) films were introduced to investigate the distance-dependent study of SPCE (40), which can be considered an attempt to obtain a uniform coupling effect for molecules at defined spatial distributions. In this study, the investigators determined the distance between the fluorophores and the metal surface by depositing stearic acid in different numbers of layers. The long chain of the amphiphilic cyanine dye DiI was deposited as the top monolayer. All the dyes were placed in a uniform position that could be controlled by designing the layers of LB films as spacers. Another advantage of this system is that all the dyes were structured so that the transition dipoles were oriented parallel to the metal surface.

Although the coupling effect for the horizontal orientation is not high, it still represents great progress in that it provides important information about interactions between the fluorophores and the metal surface, eliminating the effect of dipole orientation. The maximum intensity of SPCE occurred approximately 20 nm from the surface. LB spacing is a promising way to confirm

the uniform distribution and the uniform coupling effect of fluorophores along the normal to the metal surface. Furthermore, this study revealed that control of the coupling effect between fluorophores and a metal surface through the deposition of LB films as spacers can be achieved.

E-SPCE: electric field–assisted surface plasmon–coupled emission

The electric field at the interface is also highly localized and distance dependent. The effective distance is almost at the nanometer level and overlaps the range in which SPCE occurs. One can utilize the electric field to control the distribution or conformation of charged molecules near the surface, which would satisfy the uniform and optimum coupling effect in assays. On the basis of these considerations, we introduced the concept of electric field–assisted SPCE (E-SPCE) (64). We chose DNA, a negatively charged molecule, as a model with which to illustrate spatial coupling control in E-SPCE. Using this technique, we detected the signals of fluorophores labeled with DNA duplexes attached to a gold surface. With the assistance of an external electric field, we achieved control of the interfacial molecular conformation with DNA standing at a negative potential and lying at a positive potential so that the coupling efficiency between the dyes and the metal surface was affected by the potential. The signals were stronger at a more negative potential over the defined range, which suggested that the coupling efficiency increased with a more perpendicular orientation of DNA layers. Also, the increased signals were stronger for the longer DNA chain at the same potential, confirming that the signal changes were correlated to the conformation of DNA. The coupling efficiency increased as the labeled dyes departed from the surface with DNA duplexes oriented perpendicularly at a negative potential. Thus, larger conformational changes with longer chains produced stronger signal responses in distance-sensitive detection. However, low fluorescence at positive potentials with labeled DNA adsorbed to the metal surface. These findings show that coupling efficiency can be controlled spatially in an active way, which provides a good way to improve the manipulation of nanometer-scale processes.

4.4. Improving Optical Imaging on the Basis of Surface Plasmon–Coupled Emission

The attractive characteristics of SPCE, namely its high collection efficiency and low background noise, provide excellent performance in optical imaging. There has been increased interest in combining imaging techniques with SPCE.

Considering the well-developed optical components of microscopic equipment, SPCE imaging can be readily implemented. As is well known, in total internal reflection fluorescence (TIRF) microscopic systems, a TIRF objective with a high numerical aperture is used. Such an objective can also act as a prism with a high refractive index to ensure that the wave vectors match. Therefore, a TIRF microscope can be rebuilt as an SPCE microscope, which is known as a surface plasmon–assisted microscope (SPAM) (65, 66). The light beam excites the fluorophores at the SPR angle through the objective, and the emission is collected through the same objective at the SPCE angle. The optical design of the inverted microscopic detection can be considered as a KR configuration (65, 67). Utilizing SPCE microscopy, investigators have imaged muscle fibrils and studied the dynamics of the interactions between actin and myosin cross-bridges. With the background suppression and the selective excitation in the near field, one can focus the detection zone to follow the motion of 12 actin protomers in a muscle filament (67).

In SPCE, the detection volume is a product of evanescent-wave penetration depth and distance-dependent coupling, so a minimized detection volume of 1 to 2 al can be expected, assuming a 50-nm effective coupling depth and a 200-nm lateral diffraction limit (65, 67). This shallow detection volume is useful for the study of molecular dynamics based on fluorescence correlation spectroscopy (FCS) (68). Also, due to the enhancement effect, even the fluorescence of a single molecule can be detected with a good signal-to-noise ratio in the detection volume (69).

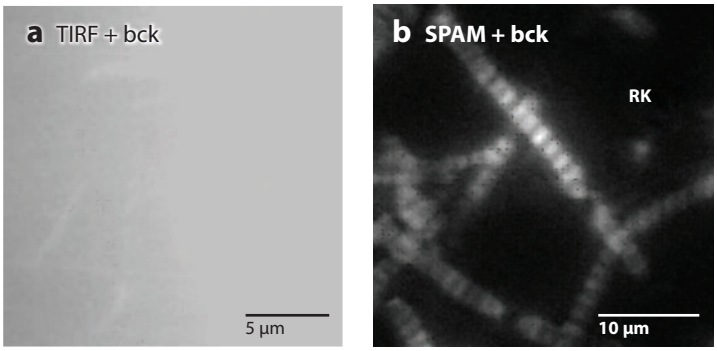

Figure 4

Myofibrils labeled with 100 nM of Alexa647-phalloidin in the presence of 0.5 mM of Rhodamine 800 as the background (bck) measured in (*a*) a conventional total internal reflection fluorescence (TIRF) microscope and (*b*) in a reverse Kretschmann surface plasmon–assisted microscope (RK-SPAM). Adapted from Reference 66. Copyright 2010, Society of Photo-Optical Instrumentation Engineers.

The implementation of a RK-SPCE microscope was expected to be simple, given that there is no need for precise incident angle adjustments (66). In the RK configuration, light directly illuminates the sample side without requiring angle adjustment or polarization, thereby reducing loss of incident intensity. As shown in **Figure 4**, myofibrils could not be imaged in a conventional TIRF microscope under high background. On the contrary, a clear image was obtained with a SPAM. On the basis of the RK-SPCE-FCS microscopy technique, the authors of this study (66) measured the kinetics of a single cross-bridge in familial hypertrophic cardiomyopathy heart muscle by monitoring the fluorescently labeled actin. These authors also observed statistically significant differences between wild and mutated heart muscle.

The point spread function of microscopic SPCE has been investigated. Lateral resolution approaching 100 nm can be observed under standing-wave excitation (70) with the numerical method or spiral phase plate to convert the point spread function into a single-lobe structure (71). Two-photon excited fluorescence has also been introduced into the imaging process. In this experiment, the authors measured the multiple colorful SPCE circles with high collection efficiency by optimizing the silver thickness (72).

In other designs, leakage radiation microscopy (LRM) was used to obtain direct images of SPCE (73). A clear SPCE ring can be observed with a Fourier transfer of the image plane in LRM. Furthermore, this technique allows the propagation of the surface plasmon polaritons to be imaged, which cannot be done in a prism-based setup. Using SPCE-LRM, investigators found that an SPCE ring displays different intensity patterns with different dielectric shapes and that the intensity distribution is affected by the illumination location on the shaped films. These findings offer a new way to control the collection efficiency at imaging and sensing (74). The supercritical angle fluorescence platform can also be modified for SPCE (75).

Surface plasmon polaritons: electromagnetic excitations that propagate at the interface between a dielectric and a conductor

5. APPLICATIONS OF SURFACE PLASMON–COUPLED EMISSION IN ANALYSIS

The great demand for reliable and sensitive detection of various objects, especially complex biological entities, has fueled analytical research. SPCE can be used in, among other applications, nucleic acid sensing, protein sensing, and other chemical sensing with fluorescence.

5.1. DNA Sensing

In SPCE, DNA hybridization was first measured between fluorophore-labeled DNA targets and surface-bound capture oligomers (76). If fluorophore-labeled DNA oligomers are complementary, they localize near the metal surface after hybridization, and a dramatic increase in fluorescence can be observed. In contrast, noncomplementary fluorophore-labeled DNA oligomers do not cause changes in SPCE. As a result, SPCE can effectively detect DNA on the basis of the change in probe localization that occurs upon hybridization, which induces efficient coupling with metal. Another advantage of SPCE in DNA detection is the effective rejection of the background signal arising from molecules that are not bound to the surface. Due to the distance-dependent coupling, the influence from fluorophores that are more distant from the surface can be eliminated. Additionally, illumination in the KR configuration can preferentially localize the excitation to regions near the metal surface. The evanescent field in the KR configuration has been amplified to yield a signal much stronger than that obtained in the RK configuration (16).

MA-SPCE offers an alternative approach to current DNA detection that satisfies the requirements of speed and sensitivity (58). In one study, the hybridization of a fluorophore-labeled target oligo with an anchor probe on a gold film under microwave heating resulted in obvious fluorescence in MA-SPCE within 1 min; in SPCE, approximately 4 h are usually required to obtain a comparative signal at room-temperature incubation. The high speed of DNA sensing is attributed to the design of the small gold disk, which is not affected by dielectric breakdown under low-power microwave. A temperature gradient is created along the disk, which causes a larger influx of complementary DNA toward the anchor probe–modified surface. The detection was achieved in whole-blood samples without the need for extra separation steps. Also, the DNA was not modified under low-power microwave, which allowed for identical fluorescence intensities after melting and rehybridization and, thus, ideal reversibility.

To improve the sensitivity and selectivity of DNA-hybridization assays, we developed a DNA sensor with label-hairpin DNA as the capture in an E-SPCE system for the highly sensitive detection of a label-free DNA target (64). In this experiment, hairpin DNA probes labeled with fluorescent dyes were attached to a gold surface, then exposed to a solution of single-stranded DNA chains. If a strand has a sequence that matches the probe, the hairpin unfolds and forms a twinned duplex that positions the fluorescent dye a few nanometers away from the surface. One would expect that the dyes strongly interact with oscillating surface plasmons and fire off an amplified fluorescence signal. In practice, however, DNA duplexes anchored to the surface may form a slanted or random orientation leading to the labeled fluorophores close to the surface, which limits the efficiency of enhancement and results in potential signal deviation with an unpredictable orientation. In addition, the duplex formation involving a single-base mismatch may also enhance the fluorescence signal in SPCE, resulting in false-positive detection. We found that E-SPCE can be used to effectively resolve these problems. With the assistance of an appropriate negative potential, the hybrids with matched DNA stood straight up in a uniform way, ensuring that all the labeled fluorophores were located in the enhancement zone to the greatest possible extent. However, most of the fluorophores were still close to the surface in the mismatched situation because the mismatched duplexes were less stable and the reaction was hindered at the repulsive potential. By actively modulating the conditions locally at the interface, with the synergistic effect of amplifying the right signal and suppressing the wrong signal, E-SPCE can be successfully used in sensitive DNA sensing, with high (up to 20-fold) discriminatory capacity for a single-base mutation in a wide range of concentrations (**Figure 5**). This technique is easy to apply to various distance-sensitive surface assays and may help create a new generation of miniaturized high-performance sensing platforms, especially in chip-based microarray assays.

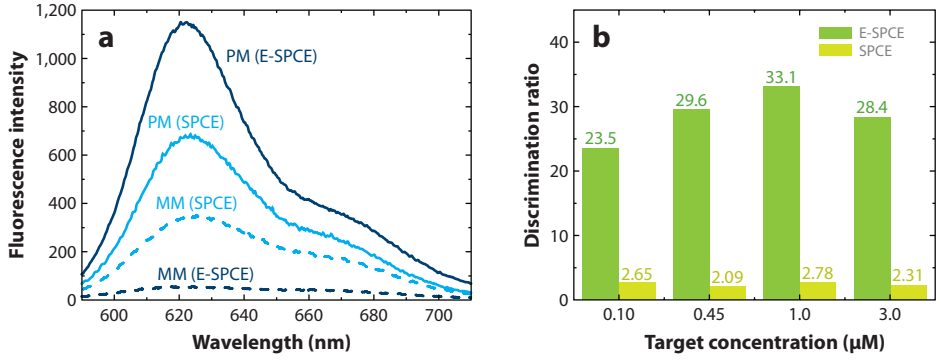

Figure 5

(*a*) Surface plasmon–coupled emission (SPCE) and electric field–assisted surface plasmon–coupled emission (E-SPCE) fluorescence spectra of hairpin DNA responding to 3.0 μM perfect matches (PM) and single-base mismatches (MM). (*b*) Discrimination ratios with target concentrations ranging from 0.10 μM to 3.0 μM PM measured in SPCE and E-SPCE. Reprinted with permission from Reference 64. Copyright 2011, American Chemical Society.

5.2. Aptamer-Based Protein Sensing

Aptamers are single-stranded nucleic acids that possess unique binding characteristics relative to their targets. Numerous high-affinity and highly specific aptamers have been selected against a wide variety of target molecules, including proteins. The configurations of aptamers are specific for the process of binding targets (77). Considering the conformational changes of aptamers before and after they bind proteins, which can cause distance changes in labeled fluorophores, we expect protein assays based on the distance-dependent coupling effect in SPCE to be developed. We designed a molecular beacon aptamer with a fluorophore labeled on its end. In the absence of the target thrombin, the immobilized aptamer formed the stem; the fluorophore was brought in close proximity to the metal, resulting in the quenching of fluorescence. Therefore, no signal was detected by SPCE. Upon thrombin binding, the distance between the fluorophore and the gold surface increased due to the conformational change in the aptamer (**Figure 6*a***) (78). However, the change in DNA conformation may not be large enough to extend from the quenching zone to the enhancement zone. In that case, the conformational change after binding to the target is only approximately 2 nm, whereas the quenching effect dominates around 5 nm from the surface. For this reason, we designed a monomolecular layer of avidin to link to the aptamer, which required the labeled fluorophore to be placed on the critical zone between quenching and coupling. Consequently, we obtained a sensitive response following the conformational change of the aptamer extending to the enhancement zone through binding to the target. The fluorescence was sharply distributed at 45°, and the SPCE signal was approximately sixfold greater than that from spontaneous FSE; undesired scattering of light from the light source was suppressed (**Figure 6*b*,*c***). This experiment proves that the combination of quenching and coupling for sensing purposes is effective. This design holds potential for the development of efficient biosensors based on conformational-switching signaling aptamers.

5.3. Immunological Detection

Immunoassays based on fluorescence are one important way to achieve highly sensitive detection of biomarkers through the specific recognition of antigens with antibodies. SPCE provides increased sensitivity and background rejection, enhancing detection in immunoassays. In SPCE, successful affinity assays have been reported in an antigen–reporter antibody (fluorophore-labeled)

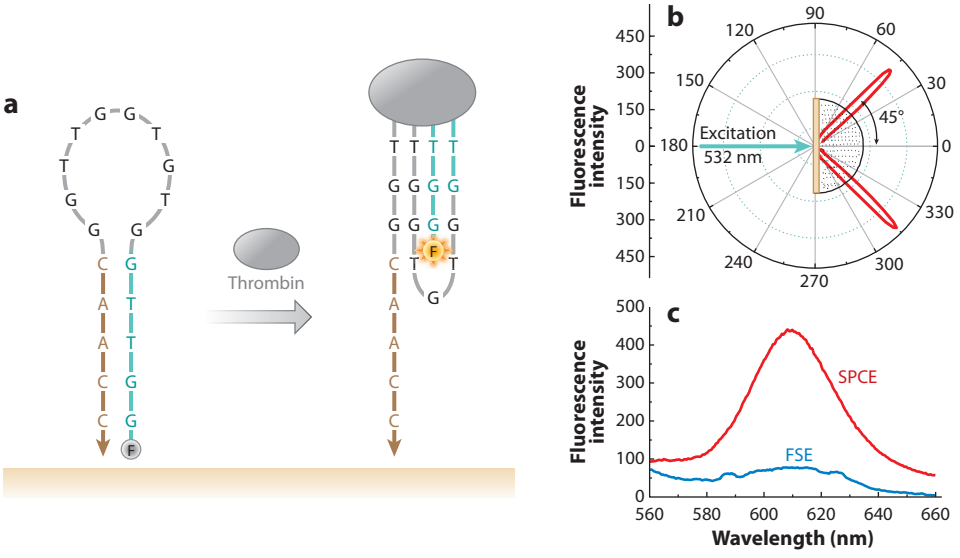

Figure 6

(*a*) The working principle of surface plasmon–coupled emission (SPCE), based on a conformational-switching signaling aptamer. When the target thrombin is added, the fluorophore is displaced into the enhancement zone. (*b*) The angular distribution of the signaling aptamer after the addition of thrombin. (*c*) The spectrum of SPCE and free-space emission (FSE) after the addition of thrombin. Adapted from Reference 78. Reproduced with permission from the Royal Society of Chemistry.

format and a capture antibody–antigen–reporter antibody (fluorophore-labeled) sandwich assay (28, 79–80). The interactions between the proteins near the interface were sensitively monitored with SPCE measurements. Moreover, the protein layer on the interface effectively acted as a spacer layer because the average protein dimension was a few nanometers, eliminating the quenching effect (81). After reaction and the critical rinsing step, directional and polarized emission was observed; the intensities indicated the different concentrations of antigens, and the binding kinetics was also detected in the defined direction because only the fluorophores labeled to the antibodies bound to the antigens on the surface could be coupled with surface plasmons. The background of the unbound regents and the autofluorescence from the sample were suppressed due to their distance from the surface, and the optically dense media in sample matrices, such as serum and whole blood, did not attenuate the SPCE signal in assays (82). This result may allow for the performance of immunoassays without separation steps even when using a complex sample. If microwave is employed, one can expect a fast and sensitive bioassay. Using a low-power microwave heating, Aslan et al. (56) achieved a 30-fold increase in assay kinetics, compared with the identical bioassay.

According to the directional emission in silver films, the angle at which the radiation propagates through the prism depends on the surface plasmon angle for the relevant wavelength. Therefore, one can measure multiple analytes by using multiple emission wavelengths that can be detected at individual angles. Model experiments have been performed to demonstrate multiwavelength immunoassays in SPCE (83). The antibodies were labeled with two fluorophores radiating at 595 nm and 665 nm. These antibodies were directed against antigen proteins bound to the silver surface. The emission from both labeled antibodies was strongly directional at different angles on the prism. The emission from 595 nm peaked at 71°, and the emission from 665 nm peaked at 68°. The emission from each labeled antibody occurred at a different angle on the glass prism, allowing independent measurement of the surface binding of each antibody.

Array-based (and even microarray-based) biochips represent a promising technology with which to develop a parallel assay platform for rapid and high-throughput analysis. Researchers have already performed the relevant investigations in SPCE (75): Arrays of transparent paraboloid polymer elements were coated with a thin layer of gold to facilitate SPCE in a modified system of supercritical angle fluorescence. In a model assay, a sandwich assay for human immunoglobulin G was carried out on a gold-coated 3 × 3 array biochip. The response was observed in a concentration between 2 ng ml^{-1} and 200 μg ml^{-1} with a limit of detection of 20 ng ml^{-1}. The limit of detection was reduced to 10 pg ml^{-1} through the use of an optimum bimetallic layer composed of 36 nm of silver and 10 nm of gold (84).

5.4. Other Fluorescence Analyses

On the basis of SPCE, other chemical fluorescence analyses can also be performed. Owing to the high collection efficiency in SPCE, investigators have achieved single-molecule detection (60). The simplest way to detect fluorescent molecules is to lay the objects near a metal surface, such as by spin-coating or dropping (85–86); the SPCE signal can then be obtained. Thin spacers such as silicon dioxide, LB films, and polyelectrolyte should be engineered between the fluorophores and the metal surface to protect the surface and minimize metal quenching effects (40, 48, 75).

The strong wavelength dependence of surface plasmon coupling at specific angles of observation offers great potential for the investigation of complex systems. The mixture of monomer, dimer, and higher-order aggregates of Rhodamine 6G were resolved with SPCE (87). Fluorescence emission from closely located protonated, deprotonated, and excimer species of 8-hydroxy-1,3,6-pyrene trisulfonic acid coupling into surface plasmons was easily separated and observed with an intensity enhancement of 11- to 14-fold (88).

Fluorescence resonance energy transfer efficiency was improved and the relative transfer rate increased by twofold in the presence of continuous silver films (89). The rise time of acceptor fluorescence intensity upon donor excitation was 10 times shorter in the presence of SPCE, and the acceptor emission in SPCE was completely linearly polarized (90).

The orientation of the transition dipole moment of fluorophores can be detected in SPCE, and the degree of horizontal or vertical orientation can be determined through comparison with simulations (91). Because the wave vector of surface plasmons parallel to the molecular orientation takes a larger value than that perpendicular to the molecular orientation, the spectral peak for the parallel configuration is located at a longer wavelength than that for the perpendicular configuration at the same observation angle (92).

In addition to being directly detected in SPCE, fluorophores can also be designed to behave as a sensing layer to reflect external stimulants. In a report on oxygen sensing (93), a ruthenium fluorophore was electrostatically attached to the SPCE surface as an ultrathin sensing layer. The response of the probes was due to collisional quenching by oxygen. This study detected both the fluorescence intensity and the lifetime for oxygen sensing. The responses for these two measurements were sensitive in SPCE, while the lifetime of the probes under FSE could not be resolved due to the weak signal from the thin sensing layer. Thus, SPCE-based fluorescence and lifetime measurements could lead to the development of chemical sensing devices with low cost and high sensitivity.

6. PERSPECTIVE AND CONCLUSION

The combination of fluorescence and SPR has led to a paradigm shift for both techniques. The development of instruments, devices, and sensors based on SPCE has steadily increased. The above-described processes for the emission of fluorophores are readily applicable to other sources

of molecular luminescence, such as phosphorescence, chemiluminescence, and electrochemiluminescence. The geometry of SPCE is also attracting attention from researchers in diverse research fields. For example, stimulated emission has been investigated with a similar device as the basis for a potential laser design (94), directional SERS has been observed (95), and enhanced scanning tunneling microscope light emission has been achieved through a prism at a defined angle (96). Therefore, SPCE has allowed for the creation of platforms for the intensive investigation of nanoscale optics via plasmon coupling.

However, it is worth noting the complexity of fluorophore-metal interactions, which involve both near- and far-field effects. The coupling between fluorophores and nanostructures with complex geometries is not yet well understood (60, 97). As a result, both the fundamentals and applications of SPCE require further study. The incorporation of novel nanomaterials, nanostructures, and nanooptical devices into SPCE would further improve the analytical applications of this technique and would expedite the design of low-cost and high-performance sensors. SPCE-based imaging will be an emerging technique. Integration of the unique properties of the directional emission into microarray imaging would reduce interference from cross talk and improve imaging quality. Undoubtedly, the development of SPCE platforms will influence the field of chip-based biomolecular detection and will significantly advance research in analytical sciences.

SUMMARY POINTS

1. SPCE is an optical technique that combines SPR and fluorescence. The unique characteristics of SPCE, specifically directional emission, background suppression, *p*-polarized emission, and distance-determined coupling, are useful for the analysis of biointerfaces.
2. By choosing the appropriate material as the optical surface, one can employ SPCE throughout the UV-to-IR range. The detection mode and the penetration depth can also be modulated.
3. Optical imaging based on SPCE offers a new way to improve sensitivity, suppress the background signal, and decrease the detection volume. Investigators have recorded images of surface plasmon polaritons, proteins, and bioarrays.
4. SPCE has been combined with other techniques, such as the use of nanoparticles, microwave radiation, and electric fields. Fast, easy, and highly sensitive sensing approaches have been developed.
5. SPCE has been used for DNA sensing, protein sensing, and the detection of other chemically and biologically relevant molecules. Investigators have improved sensitivity and selectivity by designing the sensors to incorporate the unique features of SPCE.

FUTURE ISSUES

1. Nanoparticles, nanofabrication, and new nanomaterials that can affect and amplify the electromagnetic field could become new strategies for improving the resonant coupling of surface plasmons, thereby enhancing the intensity of the fluorescence detected near the metal surface to meet the increasing requirements for sensitivity.
2. Further efforts to create feasible analytical platforms and analytical procedures to accelerate the applications of SPCE in practical assays are imperative.

3. SPCE instruments, including spectral and imaging devices, should be developed. In particular, SPCE-based imaging will become increasingly widely used, considering the growing demand for imaging analysis in biological and medical research.

DISCLOSURE STATEMENT

The authors are not aware of any affiliations, memberships, funding, or financial holdings that might be perceived as affecting the objectivity of this review.

ACKNOWLEDGMENTS

We acknowledge funds from the National Science Foundation of China (20975084, 20575055) and the 973 Program of China (2007CB935600). We thank Dr. Yu-Luan Chen for critical reading of this manuscript.

LITERATURE CITED

1. Nie SM, Zare RN. 1997. Optical detection of single molecules. *Annu. Rev. Biophys. Biomol. Struct.* 26:567–96
2. Anker JN, Hall WP, Lyandres O, Shah NC, Zhao J, Van Duyne RP. 2008. Biosensing with plasmonic nanosensors. *Nat. Mater.* 7:442–53
3. Willets KA, Van Duyne RP. 2007. Localized surface plasmon resonance spectroscopy and sensing. *Annu. Rev. Phys. Chem.* 58:267–97
4. Lakowicz JR. 2001. Radiative decay engineering: biophysical and biomedical applications. *Anal. Biochem.* 298:1–24
5. Neumann T, Johansson ML, Kambhampati D, Knoll W. 2002. Surface-plasmon fluorescence spectroscopy. *Adv. Funct. Mater.* 12:575–86
6. Lakowicz JR, Malicka J, Gryczynski I, Gryczynski Z. 2003. Directional surface plasmon–coupled emission: a new method for high sensitivity detection. *Biochem. Biophys. Res. Commun.* 307:435–39
7. Lakowicz JR. 2005. Radiative decay engineering. 5. Metal-enhanced fluorescence and plasmon emission. *Anal. Biochem.* 337:171–94
8. Geddes CD, Gryczynski I, Malicka J, Gryczynski Z, Lakowicz JR. 2004. Directional surface plasmon coupled emission. *J. Fluoresc.* 14:119–23
9. Lakowicz JR. 2004. Radiative decay engineering. 3. Surface plasmon–coupled directional emission. *Anal. Biochem.* 324:153–69
10. Gryczynski I, Malicka J, Gryczynski Z, Lakowicz JR. 2004. Radiative decay engineering. 4. Experimental studies of surface plasmon–coupled directional emission. *Anal. Biochem.* 324:170–82
11. Homola J, Koudela I, Yee SS. 1999. Surface plasmon resonance sensors based on diffraction gratings and prism couplers: sensitivity comparison. *Sens. Actuators B* 54:16–24
12. Kurihara K, Suzuki K. 2002. Theoretical understanding of an absorption-based surface plasmon resonance sensor based on Kretschmann's theory. *Anal. Chem.* 74:696–701
13. Homola J, Yee SS, Gauglitz G. 1999. Surface plasmon resonance sensors: review. *Sens. Actuators B* 54:3–15
14. Calander N. 2004. Theory and simulation of surface plasmon–coupled directional emission from fluorophores at planar structures. *Anal. Chem.* 76:2168–73
15. Trnavsky M, Enderlein J, Ruckstuhl T, McDonagh C, MacCraith BD. 2008. Experimental and theoretical evaluation of surface plasmon–coupled emission for sensitive fluorescence detection. *J. Biomed. Opt.* 13:054021
16. Malicka J, Gryczynski I, Gryczynski Z, Lakowicz JR. 2004. Use of surface plasmon–coupled emission to measure DNA hybridization. *J. Biomol. Screen.* 9:208–15

17. Smith DS, Kostov Y, Rao G, Gryczynski I, Malicka J, et al. 2005. First observation of surface plasmon–coupled emission due to LED excitation. *J. Fluoresc.* 15:895–900
18. Cao SH, Xie TT, Cai WP, Li YQ. 2010. Observation of surface plasmon–coupled directional fluorescence using thin iron films. *Chem. J. Chin. Univ.* 31:61–63
19. Smith DS, Kostov Y, Rao G. 2008. Signal enhancement of surface plasmon–coupled directional emission by a conical mirror. *Appl. Opt.* 47:5229–34
20. Li YQ, Xie TT, Cai WP. 2009. Surface plasma coupling fluorescence detection apparatus. *China Patent 200910111882*
21. Hung YJ, Smolyaninov II, Davis CC, Wu HC. 2006. Fluorescence enhancement by surface gratings. *Opt. Express* 14:10825–30
22. Chowdhury MH, Malyn SN, Aslan K, Lakowicz JR, Geddes CD. 2007. First observation of surface plasmon–coupled chemiluminescence (SPCC). *Chem. Phys. Lett.* 435:114–18
23. Zhang J, Gryczynski Z, Lakowicz JR. 2004. First observation of surface plasmon–coupled electrochemiluminescence. *Chem. Phys. Lett.* 393:483–87
24. Previte MJR, Aslan K, Zhang YX, Geddes CD. 2006. Surface plasmon coupled phosphorescence (SPCP). *Chem. Phys. Lett.* 432:610–15
25. Gryczynski I, Malicka J, Lakowicz JR, Goldys EM, Calander N, Gryczynski Z. 2005. Directional two-photon induced surface plasmon–coupled emission. *Thin Solid Films* 491:173–76
26. Mondal PP, Gilbert RJ, So PTC. 2008. Plasmon enhanced fluorescence microscopy below quantum noise limit with reduced photobleaching effect. *Appl. Phys. Lett.* 93:093901
27. Gryczynski I, Malicka J, Gryczynski Z, Lakowicz JR. 2004. Surface plasmon–coupled emission with gold films. *J. Phys. Chem. B* 108:12568–74
28. Lakowicz JR, Malicka J, Matveeva E, Gryczynski I, Gryczynski Z. 2005. Plasmonic technology: novel approach to ultrasensitive immunoassays. *Clin. Chem.* 51:1914–22
29. Hiep HM, Fujii M, Hayashi S. 2007. Effects of molecular orientation on surface-plasmon-coupled emission patterns. *Appl. Phys. Lett.* 91:183110
30. Penninck L, Mladenowski S, Neyts K. 2010. The effects of planar metallic interfaces on the radiation of nearby electrical dipoles. *J. Opt.* 12:075001
31. Gryczynski I, Malicka J, Nowaczyk K, Gryczynski Z, Lakowicz JR. 2004. Effects of sample thickness on the optical properties of surface plasmon–coupled emission. *J. Phys. Chem. B* 108:12073–83
32. Gryczynski I, Malicka J, Nowaczyk K, Gryczynski Z, Lakowicz JR. 2006. Waveguide-modulated surface plasmon–coupled emission of Nile blue in poly(vinyl alcohol) thin films. *Thin Solid Films* 510:15–20
33. Salamon Z, Macleod HA, Tollin G. 1997. Coupled plasmon-waveguide resonators: a new spectroscopic tool for probing proteolipid film structure and properties. *Biophys. J.* 73:2791–97
34. Salamon Z, Tollin G. 2001. Optical anisotropy in lipid bilayer membranes: coupled plasmon-waveguide resonance measurements of molecular orientation, polarizability, and shape. *Biophys. J.* 80:1557–67
35. Calander N. 2005. Surface plasmon–coupled emission and Fabry-Pérot resonance in the sample layer: a theoretical approach. *J. Phys. Chem. B* 109:13957–63
36. Barnes WL. 1998. Fluorescence near interfaces: the role of photonic mode density. *J. Mod. Opt.* 45:661–99
37. Hellen EH, Axelrod D. 1987. Fluorescence emission at dielectric and metal-film interfaces. *J. Opt. Soc. Am. B* 4:337–50
38. Weber WH, Eagen CF. 1979. Energy transfer from an excited dye molecule to the surface plasmons of an adjacent metal. *Opt. Lett.* 4:236–38
39. Ford GW, Weber WH. 1984. Electromagnetic interactions of molecules with metal surfaces. *Phys. Rep.* 113:195–287
40. Ray K, Szmacinski H, Enderlein J, Lakowicz JR. 2007. Distance dependence of surface plasmon–coupled emission observed using Langmuir-Blodgett films. *Appl. Phys. Lett.* 90:251116
41. Wang YK, Yang TY, Pourmand M, Miller JJ, Tuominen MT, Achermann M. 2010. Time-resolved surface plasmon polariton coupled exciton and biexciton emission. *Opt. Express* 18:15560–68
42. Sun YG, Xia YN. 2003. Gold and silver nanoparticles: a class of chromophores with colors tunable in the range from 400 to 750 nm. *Analyst* 128:686–91
43. Tian ZQ, Ren B, Li JF, Yang ZL. 2007. Expanding generality of surface-enhanced Raman spectroscopy with borrowing SERS activity strategy. *Chem. Commun.* 43:3514–34

44. Stiles PL, Dieringer JA, Shah NC, Van Duyne RP. 2008. Surface-enhanced Raman spectroscopy. *Annu. Rev. Anal. Chem.* 1:601–26
45. Aslan K, Geddes CD. 2009. Directional surface plasmon coupled luminescence for analytical sensing applications: which metal, what wavelength, what observation angle? *Anal. Chem.* 81:6913–22
46. Previte MJR, Zhang YX, Aslan K, Geddes CD. 2007. Surface plasmon coupled fluorescence from copper substrates. *Appl. Phys. Lett.* 91:151902
47. Gryczynski I, Malicka J, Gryczynski Z, Nowaczyk K, Lakowicz JR. 2004. Ultraviolet surface plasmon–coupled emission using thin aluminum films. *Anal. Chem.* 76:4076–81
48. Aslan K, Previte MJR, Zhang YX, Geddes CD. 2008. Surface plasmon coupled fluorescence in the ultraviolet and visible spectral regions using zinc thin films. *Anal. Chem.* 80:7304–12
49. Aslan K, Geddes CD. 2009. Surface plasmon coupled chemiluminescence from zinc substrates: directional chemiluminescence. *Appl. Phys. Lett.* 94:073104
50. Aslan K, Weisenberg M, Hortle E, Geddes CD. 2009. Surface plasmon coupled chemiluminescence from iron thin films: directional and approaching fixed angle observation. *J. Appl. Phys.* 106:014131
51. Aslan K, Zhang YX, Geddes CD. 2009. Directional, broad, and fixed angle surface plasmon coupled fluorescence from iron thin films. *J. Phys. Chem. C* 113:20535–38
52. Aslan K, Zhang YX, Geddes CD. 2009. Surface plasmon coupled fluorescence in the visible to near-infrared spectral regions using thin nickel films: application to whole blood assays. *Anal. Chem.* 81:3801–8
53. Ray K, Chowdhury MH, Lakowicz JR. 2008. Observation of surface plasmon–coupled emission using thin platinum films. *Chem. Phys. Lett.* 465:92–95
54. Aslan K, Weisenberg M, Hortle E, Geddes CD. 2009. Fixed-angle observation of surface plasmon coupled chemiluminescence from palladium thin films. *Appl. Phys. Lett.* 95:123117
55. Weisenberg M, Aslan K, Hortle E, Geddes CD. 2009. Directional surface plasmon coupled chemiluminescence from nickel thin films: fixed angle observation. *Chem. Phys. Lett.* 473:120–25
56. Aslan K, Malyn SN, Geddes CD. 2007. Microwave-accelerated surface plasmon–coupled directional luminescence: application to fast and sensitive assays in buffer, human serum and whole blood. *J. Immunol. Methods* 323:55–64
57. Aslan K, Geddes CD. 2005. Microwave-accelerated metal-enhanced fluorescence: platform technology for ultrafast and ultrabright assays. *Anal. Chem.* 77:8057–67
58. Aslan K, Previte MJR, Zhang Y, Geddes CD. 2008. Microwave-accelerated surface plasmon–coupled directional luminescence. 2. A platform technology for ultra fast and sensitive target DNA detection in whole blood. *J. Immunol. Methods* 331:103–13
59. Previte MJR, Geddes CD. 2007. Microwave-triggered surface plasmon coupled chemiluminescence. *J. Am. Chem. Soc.* 129:9850–51
60. Lakowicz JR, Ray K, Chowdhury M, Szmacinski H, Fu Y, et al. 2008. Plasmon-controlled fluorescence: a new paradigm in fluorescence spectroscopy. *Analyst* 133:1308–46
61. Previte MJR, Aslan K, Zhang YX, Geddes CD. 2007. Metal-enhanced surface plasmon–coupled phosphorescence. *J. Phys. Chem. C* 111:6051–59
62. Chowdhury MH, Ray K, Geddes CD, Lakowicz JR. 2008. Use of silver nanoparticles to enhance surface plasmon–coupled emission (SPCE). *Chem. Phys. Lett.* 452:162–67
63. Aslan K, McDonald K, Previte MJR, Zhang YX, Geddes CD. 2008. Silver island nanodeposits to enhance surface plasmon coupled fluorescence from copper thin films. *Chem. Phys. Lett.* 464:216–19
64. Cao SH, Xie TT, Cai WP, Liu Q, Li YQ. 2011. Electric field assisted surface plasmon–coupled directional emission: an active strategy on enhancing sensitivity for DNA sensing and efficient discrimination of single base mutation. *J. Am. Chem. Soc.* 133:1787–89
65. Gryczynski Z, Borejdo J, Calander N, Matveeva EG, Gryczynski I. 2006. Minimization of detection volume by surface-plasmon-coupled emission. *Anal. Biochem.* 356:125–31
66. Mettikolla P, Calander N, Luchowski R, Gryczynski I, Gryczynski Z, Borejdo J. 2010. Kinetics of a single cross-bridge in familial hypertrophic cardiomyopathy heart muscle measured by reverse Kretschmann fluorescence. *J. Biomed. Opt.* 15:017011
67. Borejdo J, Gryczynski Z, Calander N, Muthu P, Gryczynski I. 2006. Application of surface plasmon coupled emission to study of muscle. *Biophys. J.* 91:2626–35

68. Borejdo J, Calander N, Gryczynski Z, Gryczynski I. 2006. Fluorescence correlation spectroscopy in surface plasmon coupled emission microscope. *Opt. Express* 14:7878–88
69. Stefani FD, Vasilev K, Bocchio N, Stoyanova N, Kreiter M. 2005. Surface-plasmon-mediated single-molecule fluorescence through a thin metallic film. *Phys. Rev. Lett.* 94:023005
70. Chung E, Kim YH, Tang WT, Sheppard CJR, So PTC. 2009. Wide-field extended-resolution fluorescence microscopy with standing surface-plasmon resonance waves. *Opt. Lett.* 34:2366–68
71. Tang WT, Chung E, Kim YH, So PTC, Sheppard CJR. 2010. Surface-plasmon-coupled emission microscopy with a spiral phase plate. *Opt. Lett.* 35:517–19
72. Chiu KC, Lin CY, Dong CY, Chen SJ. 2011. Optimizing silver film for surface plasmon–coupled emission induced two-photon excited fluorescence imaging. *Opt. Express* 19:5386–96
73. Zhang DG, Yuan XC, Bouhelier A. 2010. Direct image of surface-plasmon-coupled emission by leakage radiation microscopy. *Appl. Opt.* 49:875–79
74. Zhang DG, Moh KJ, Yuan XC. 2010. Surface plasmon–coupled emission from shaped PMMA films doped with fluorescence molecules. *Opt. Express* 18:12185–90
75. Yuk JS, Trnavsky M, McDonagh C, MacCraith BD. 2010. Surface plasmon–coupled emission (SPCE)-based immunoassay using a novel paraboloid array biochip. *Biosens. Bioelectron.* 25:1344–49
76. Malicka J, Gryczynski I, Gryczynski Z, Lakowicz JR. 2003. DNA hybridization using surface plasmon–coupled emission. *Anal. Chem.* 75:6629–33
77. Cho EJ, Lee JW, Ellington AD. 2009. Applications of aptamers as sensors. *Annu. Rev. Anal. Chem.* 2:241–64
78. Xie TT, Liu Q, Cai WP, Chen Z, Li YQ. 2009. Surface plasmon–coupled directional emission based on a conformational-switching signaling aptamer. *Chem. Commun.* 45:3190–92
79. Matveeva E, Gryczynski Z, Gryczynski I, Malicka J, Lakowicz JR. 2004. Myoglobin immunoassay utilizing directional surface plasmon–coupled emission. *Anal. Chem.* 76:6287–92
80. Matveeva E, Gryczynski Z, Gryczynski I, Lakowicz JR. 2004. Immunoassays based on directional surface plasmon–coupled emission. *J. Immunol. Methods* 286:133–40
81. Yuk JS, McDonagh C, MacCraith BD. 2010. Demonstration of a surface plasmon–coupled emission (SPCE)-based immunoassay in the absence of a spacer layer. *Anal. Bioanal. Chem.* 398:1947–54
82. Matveeva EG, Gryczynski I, Barnett A, Calander N, Gryczynski Z. 2007. Red blood cells do not attenuate the SPCE fluorescence in surface assays. *Anal. Bioanal. Chem.* 388:1127–35
83. Matveeva E, Malicka J, Gryczynski I, Gryczynski Z, Lakowicz JR. 2004. Multi-wavelength immunoassays using surface plasmon–coupled emission. *Biochem. Biophys. Res. Commun.* 313:721–26
84. Yuk JS, MacCraith BD, McDonagh C. 2011. Signal enhancement of surface plasmon–coupled emission (SPCE) with the evanescent field of surface plasmons on a bimetallic paraboloid biochip. *Biosens. Bioelectron.* 26:3213–18
85. Gryczynski I, Malicka J, Jiang W, Fischer H, Chan WCW, et al. 2005. Surface-plasmon-coupled emission of quantum dots. *J. Phys. Chem. B* 109:1088–93
86. Kostov Y, Smith DS, Tolosa L, Rao G, Gryczynski I, et al. 2005. Directional surface plasmon-coupled emission from a 3 nm green fluorescent protein monolayer. *Biotechnol. Progr.* 21:1731–35
87. Sathish S, Kostov Y, Rao G. 2009. High-resolution surface plasmon coupled resonant filter for monitoring of fluorescence emission from molecular multiplexes. *Appl. Phys. Lett.* 94:223113
88. Sathish RS, Kostov Y, Rao G. 2009. Spectral resolution of molecular ensembles under ambient conditions using surface plasmon coupled fluorescence emission. *Appl. Opt.* 48:5348–53
89. Szmacinski H, Ray K, Lakowicz JR. 2009. Effect of plasmonic nanostructures and nanofilms on fluorescence resonance energy transfer. *J. Biophoton.* 2:243–52
90. Jankowski D, Bojarski P, Kwiek P, Rangelowa-Jankowska S. 2010. Donor-acceptor nonradiative energy transfer mediated by surface plasmons on ultrathin metallic films. *Chem. Phys.* 373:238–42
91. Frischeisen J, Yokoyama D, Adachi C, Brutting W. 2010. Determination of molecular dipole orientation in doped fluorescent organic thin films by photoluminescence measurements. *Appl. Phys. Lett.* 96:073302
92. Ghazali FAM, Fujii M, Hayashi S. 2009. Anisotropic propagation of surface plasmon polaritons caused by oriented molecular overlayer. *Appl. Phys. Lett.* 95:033303
93. Smith DS, Kostov Y, Rao G. 2007. SPCE-based sensors: ultrafast oxygen sensing using surface plasmon–coupled emission from ruthenium probes. *Sens. Actuators B* 127:432–40

94. Noginov MA, Zhu G, Mayy M, Ritzo BA, Noginova N, Podolskiy VA. 2008. Stimulated emission of surface plasmon polaritons. *Phys. Rev. Lett.* 101:226806
95. Meyer SA, Le Ru EC, Etchegoin PG. 2011. Combining surface plasmon resonance (SPR) spectroscopy with surface-enhanced Raman scattering (SERS). *Anal. Chem.* 83:2337–44
96. Ahamed JU, Sanbongi T, Katano S, Uehara Y. 2010. Prism-coupled scanning tunneling microscope light emission spectroscopy of Au film covered with self-assembled alkanethiol monolayer. *Jpn. J. Appl. Phys.* 49:08LB09
97. Fort E, Gresillon S. 2008. Surface enhanced fluorescence. *J. Phys. D* 41:013001

Annual Review of
Analytical Chemistry

Volume 5, 2012

Contents